Rapid Detection of Trace Bacteria in Biofluids Using Porous Monoliths in Microchannels

Junyu Mai[a], **Vinay V. Abhyankar**[a], **Matthew E. Piccini**[a], **Juan P. Olano**[b], **Richard Willson**[c], and **Anson V. Hatch**[a,*]

[a]Department of Biotechnology and Bioengineering, Sandia National Laboratories, 7011 East Ave., Livermore, CA 94551, USA.

[b]University of Texas Medical Branch, 301 University Blvd, Galveston, TX 77555, USA

[c]University of Houston, 4800 Calhoun Rd, Houston, TX 77004, USA

Abstract

We present advancements in microfluidic technology for rapid detection of as few as ten rickettsial organisms in complex biological samples. An immuno-reactive filter, macroporous polyacrylamide monolith (PAM), fabricated within a microfluidic channel enhances solid-phase immuno-capture, staining and detection of targeted bacteria. Bacterial cells in samples flowing through the channel are forced to interact with the PAM filter surface due to size exclusion, overcoming common transport and kinetic limitations for rapid (minutes), high-efficiency (~100%) capture. In the process, targeted cells in sample volumes of 10 μl to >100 μl are concentrated within a sub-50 nl region at the PAM filter edge in the microchannel, thus concentrating them over 1,000-fold. This significantly increases sensitivity, as the hydrophilic PAM also yields low non-specific immuno-fluorescence backgrounds with samples including serum, blood and non-targeted bacteria. The concentrated target cells are detected using fluorescently-labeled antibodies. With a single $2.0 \times 2.0 \times 0.3$ mm PAM filter, as few as 10 rickettsial organisms per 100 μl of lysed blood sample can be analyzed within 60 min, as compared to hours or even days needed for conventional detection methods. This method is highly relevant to rapid, multiplexed, low-cost point of care diagnostics at early stages of infection where diagnostics providing more immediate and actionable test results are needed to improve patient outcomes and mitigate potential natural and non-natural outbreaks or epidemics of rickettsial diseases.

Keywords

Blood borne bacteria detection; microfluidic device; point-of-care diagnostic assay; polyacrylamide monolith; macroporous monolith filter; *Rickettsia* detection

---

* Corresponding author, PO Box 969, Mail Stop 9291, 7011 East Ave., Sandia National Laboratories, Livermore, CA 94551, USA. Phone number: (925)294-6291 ahatch@sandia.gov.

1. Introduction

The ability to accurately diagnose potentially lethal infectious diseases at or even before their early symptomatic stages of disease remains a high priority due to risks of natural or unnatural outbreaks or epidemics. For the most threatening diseases, diagnostic tests are largely limited to confirmatory use because the time needed for a lab diagnosis test is too long for point-of-care therapeutic intervention. More immediate, actionable test methods are needed for early diagnosis. As one of the most dangerous bacteria that can cause life-threatening diseases in humans, Rickettsial bacteria are an endemic problem in regions across the globe, and attempts to develop a rickettsiae-based bioweapon have also been documented (Azad 2007). Historically, rickettsiae have been divided into typhus group (TG) and spotted fever group (SFG). The former only has two members, namely *R. prowazekii* and *R. typhi*, the agents of epidemic and endemic typhus, respectively. On the other hand the SFG has several members including *R. rickettsii* and *R. conorii*, the agents of Rocky Mountain spotted fever and other spotted fevers in the Americas and Mediterranean spotted fever, respectively (Nyka 1950). If prompt and accurate diagnosis is rendered, rickettsial infections can be successfully treated using early and adequate antibiotic therapy. The drug of choice for rickettsial infections is doxycycline, followed by other tetracyclines. Unfortunately, these antibiotics are seldom used as empiric therapy in clinical settings for other undifferentiated febrile illnesses. In fact, some of the antimicrobial agents such as sulfonamides used in the clinical setting can worsen the clinical course of human rickettsioses. (Chapman 2006; Moody and Chiodini 2000). The acute phase of all rickettsioses occurs mostly as an undifferentiated febrile illness difficult to distinguish from other more common febrile conditions, leading to the use of ineffective antimicrobial therapy which eventually leads to either a fatal outcome or a more prolonged and severe clinical course (Chapman 2006). Current diagnostics primarily serve as confirmatory testsafter treatment choices have been made (Chapman 2006; Moody and Chiodini 2000). To be most useful, point-of-care diagnostic assays for rickettsial diseases must be rapid (sample-to-answer time <1 hr), highly sensitive, specific and affordable.

A number of technical challenges must be addressed to provide actionable results in time to support treatment decisions. The current gold standard is detection of rising serum antibody titers in paired sera (acute and convalescent samples obtained in at least a two weeks interval) by indirect immunofluorescence antibody (IFA) assay. However, this technique has a low clinical sensitivity during the acute phase and therefore appropriate therapeutic selections cannot be made timely. We focus instead on capturing rickettsial organisms using sandwich immunoassays with antibodies raised against *R. conorii* and *R. typhi*. The ultimate goal is to detect circulating rickettsial organisms in human blood during the acute phase of the disease. Existing antigen-capture or direct pathogen test methods are low to moderately sensitive and can be lengthy and costly, and usually require biohazard safety level 3 (BSL-3) facilities and highly trained personnel. Immunohistochemical (IHC) staining of antigens in skin biopsy specimens (Walker 1995) is highly specific and acceptably sensitive, but requires several hours of labor and an experienced pathologist. Nucleic acid detection by polymerase chain reaction (PCR) or real-time PCR is highly specific and acceptably sensitive for whole blood specimens but requires labor-intensive sample preparation

(Eremeeva et al. 2003; Jiang et al. 2003; Stenos et al. 2005). Special shell-vial cell culture assays have been developed for diagnosis of rickettsioses, but 4-15 days of culture in a BSL-3 facility is needed (Birg et al. 1999; La Scola and Raoult 1996; Quesada et al. 2006).

Here, we describe advancements in microfluidic biosensor technology addressing key requirements for high detection sensitivity and specificity, in a test format poised for rapid, simple and affordable use in point-of-care settings. As a proof of concept, we demonstrate detection of rickettsial organisms in complex biological samples including serum, blood and high backgrounds of non-targeted bacteria. We developed an immuofluorescence-based rickettsial detection assay using an antibody-coated macroporous polyacrylamide monolith (PAM) fabricated within a microfluidic channel to capture and concentrate bacteria from blood samples. Porous polymer monoliths have been explored for wide-ranging uses in microfluidic applications including filtration, pumping and chromatography (Namera et al. 2011; Svec 2010; Vázquez and Paull 2010). Acrylamide-based monoliths were previously explored for capillary electrochromatography (Gury a et al. 2007; Palm and Novotny 1997; Svec 2010; Xie et al. 1997). Here, the antibody-functionalized PAM filter enables highly effective immunocapture and sensitive detection of rickettsial organisms in a flow-through format (Figure 1). The PAM exhibits low non-specific background from potentially interfering blood components and non-targeted bacterial species. Performance of the device is demonstrated using serum and blood samples spiked with known quantities of *R. typhi* and *R. conorii*. With spatially resolved fluorescent imaging, individual particles were counted with a detection limit of ~10^2 cells/ml and linear range up to over 10^5 cells/ml biofluid . A 10 μl sample can be analyzed in about 30 min and larger volumes processed if desired. For acute phase human rickettsioses, the range of rickettsial organisms found in blood circulation is not well defined. A significant technical concern in developing an actionable early diagnostic test is that blood sampling for acute phase diagnostics may require an assay detection limit of as few as ~10 bacteria in a relatively large volume of blood (~0.1 to 1 ml). The methods described were developed with the aim of meeting these potential sampling and high sensitivity requirements in addition to affordability, and usability criteria for point of care settings.

2. Material and methods

2.1 Reagents and materials

N,N'-methylenebisacrylamide (bisacrylamide), streptavidin acrylamide, and Alexa Fluor 647 microscale protein labeling kit were from Invitrogen (Calsbad, CA). 40% Acrylamide solution, 3-(trimethoxysilyl)propyl methacrylate (98%), methylcellulose (MC), sodium phosphate, N-methylformamide (NMF), N,N'-diacryloylpiperazine (PDA), tetraethylthiuram disulfide (TED) and 2,2-dimethoxy-2-phenylacetophenone (DMPA), polyethylene glycol (PEG) 8000, Saponin, Atto 488-biotin, and glacial acetic acid were from Sigma (St. Louis, MO). 2,2'-Azobis[2-methyl-*N*-(2-hydroxyethyl) propionamide] photoinitiator (VA-086) was from Wako Chemicals (Richmond, VA). Urethane diacrylate (UDA) and triethyleneglycol dimethacrylate (TEGDMA) were from Sartomer (Exton, PA). PBS buffer (20X) was from Thermo Scientific (Rockford, IL). EZ-link NHS-PEG$_4$-Biotin was from Thermo Scientific.

Pressure sensitive adhesive (PSA) tapes were from 3M (St. Paul, MN). Glass cover slips were from Fisher Scientific (Pittsburg, PA). Glass fiber filter membranes were from Sterlitech (Kent, WA).

Heat-inactivated *R. typhi* and *R. conorii* were used in all the assays. To raise polyclonal rabbit anti-*R. typhi* and anti-*R. conorii* antibodies, New Zealand rabbits were immunized with 10^6 rickettsial organisms intravenously every 3 weeks until antibody titers by IFA reached 1:2,096. The rabbits were sacrificed humanely according to IACUC protocols and blood was harvested. Serum was separated by a low-speed centrifugation step (4,000 g) and purified using high affinity columns coated with protein G. Heat-killed *Escherichia coli* O157:H7 was purchased from KPL (Gaithersburg, MD). Healthy human serum and human blood was from Innovative Research (Novi, MI).

2.2 Device fabrication

A microfluidic channel layout was fabricated by photolithographic polymerization of urethane diacrylate (UDA) microchannels between two glass coverslips as shown in Figure 2 and as previously described (Abhyankar and Hatch 2012). Two glass coverslips (24×40 mm, No. 1.5, Fisher Scientific), one with channel via of 1 mm diameter holes cut using laser cutter, and the other without, were first cleaned with methanol and then spaced by two strips of 300 μm-thick double-sided pressure sensitive adhesive (PSA) tape at the edges. For a uniformed acrylate-silane coating on the glass surface to allow subsequent covalent linkage between glass and UDA, a mixture of 2:3:5 (v/v/v) 3-(trimethoxysilyl)propyl methacrylate, glacial acetic acid, and de-ionized water was pipetted into the space between the two glass coverslips and allowed to sit for 30 min inside a sealed container. The coverslips were then rinsed twice with methanol and twice with DI water, and dried with a vacuum.

UDA monomer mixture [48.75% UDA, 48.75% triethyleneglycol dimethacrylate (TEGMDA), 1.5% 2,2-dimethoxy-2-phenylacetophenone (DMPA) and 1% Tetraethylthiuram disulfide (TED)] was prepared with 4 h stirring and mixing enhanced via sonication for 30 min. The UDA monomer solution was pipetted into the 300 μm-thick cavity between the two glass coverslips through the *via* holes on the glass coverslip by manual pipetting. Black electrical tape with laser cut channel design was placed on the cover slip and served as a lithography mask. After illumination by a collimated UV light source centered at 365 nm at 25 mW/cm^2 from a mercury lamp (OAI) (same setting for UV exposure as in the following steps) for 30 s, UDA channel wall was formed at the unmasked region inside between the coverslips. The uncured UDA monomer mixture in the masked regions (where the channels were) was removed by vacuum suction and the channels were rinsed with methanol, followed by UV post cure for another 40 s. The device and the channels were then cleaned with methanol and dried.

Our method for fabricating protein functionalized polyacrylamide monoliths extends upon earlier development of polyacrylamide monoliths (Gury a et al. 2007; Xie et al. 1997) formed from monomer solutions of buffered water/formamide/PEG/acrylamide. Here, we added photoinitiator to allow photolithographic patterning of the monolith in a microchannel and acrylamide streptavidin for simultaneous monolith functionalization for an immunoassay. The glass/UDA/glass channels were first filled with N-methylformamide

(NMF) for 1 min and then the polyacrylamide monolith monomer mixture [1 ml contained 47.5 μl 40% acrylamide solution, 30 mg N,N'-diacryloylpiperazine (PDA), 30 mg Polyethylene glycol (PEG) 8000, 1 mg streptavidin acrylamide, 2 mg VA-086 photoinitiator, and 950 μl NMF]. The channel openings were blocked with removable tape to prevent flow of monomer solution during photopolymerization of the PAM element via 100 s UV exposure through the 2mm × 2mm mask window. After the uncured monomer mixture was removed, the channels were filled with deionized H_2O and let sit for at least 2 h for complete release of uncured monomers from the PAM. The channels were further rinsed with deionized H_2O and filled with 5% linear acrylamide polymerization mixture (5% acrylamide and 2 mg/ml VA-086 in H_2O) and exposed under UV for 3 min to coat channels against non-specific adhesion of sample and reagent components.

We found PAM was effectively grafted to the silanized glass surface but not as well to the UDA edges. To enhance bonding of PAM to the UDA surface, an intermediate step was added; photopolymerization of a thin polyacrylamide gel on the UDA channel surface defined by a 2.0×0.5 mm window in the lithographic mask using a mixture of acrylamide/bisacrylamide (8%T, 10%C) with 2 mg/ml VA-086 photoinitiator. With the elastic polyacrylamide gel on the UDA wall, the PAM monomers diffused into the polyacrylamide gel and polymerized both inside and outside the polyacrylamide gel and thus effectively graft onto the UDA surface through the polyacrylamide gel. The channel openings were sealed with removable tape to prevent flow during polymerization with 45 s UV exposure. Afterwards the channels were cleaned with deionized water and exposed to UV for 30 s post cure. The channels were then ready for PAM fabrication.

To post-functionalize PAM surface with a specific antibody, devices were filled with 5 μl of 0.2 mg/ml biotinylated antibodies for 2 h at room temperature to ensure maximal binding of antibodies to the PAM through high-affinity streptavidin-biotin interaction. Antibody stock was biotinylated beforehand using EZ-link NHS-PEG$_4$-Biotin following the manufacturer's instructions. The channels were then rinsed with PBS three times and the device was ready for use. A custom laser-cut PMMA manifold for coupling chips to pumps was attached onto the glass coverslip device using double-sided adhesive tapes. Device structure and images are illustrated in Figure 2.

2.3 Assay protocols

As shown in Figure 3, samples were loaded into the device by syringe pump (New Era Pump System, Farmingdale, NY) from port a to d. Human blood samples spiked with rickettsial organisms (concentration varied from 1×10^2 to 5×10^5 cell/ml) were processed by lysing using 4 volumes of 0.2% Saponin, vortexing for 5 s, and passing through a 15 mm-long glass fiber filter membrane (1.5 μm pore size) prior to injection into the microchannel. A serum sample spiked with rickettsial organisms was loaded directly onto the device. Volumes from 10 to >100 μl can be processed depending on the concentration of targeted bacteria and the sensitivity required. In data shown in Fig. 5, a fixed sample volume of 60 μl was loaded for 30 min at 2 μl/min. PBS was subsequently pumped through port a to b for 5 min at 20 μl/min to wash non-captured sample components away from the PAM. Reporter solution, 20 nM AF647-anti-*R. typhi* antibody, was then loaded from port a to b to fill the

channel including PAM immuno-capture interface and incubated for 10 min. Afterwards, unbound reporter antibody was rinsed with PBS injection from ports a and c to b at 20 μl/min for 5 min.

Immunofluorescence results were measured by epifluorescence using a 5X objective lens and optical filter set for AF-647 fluorescence (excitation at 642 nm and emission at 705 nm) on an inverted fluorescent microscrope (Olympus). The lens was focused on the ~50 nL region of chips where targeted cells were captured at the front edge of PAM and stained by reporter antibody. Spatially resolved fluorescent images captured with a CCD camera (CoolSNAP HQ, Photometrics) were auto-analyzed using ImageJ software (http://rsbweb.nih.gov/ij/). Processing included background subtraction and threshold intensity set to count particles. Fluorescence background was measured from the fluorescent image of the same region of interest in the unstained channels.

3. Results and discussion

3.1 Characterization of PAM device

The PAM device configuration addresses a long list of diagnostic test requirements for early detection of highly virulent pathogens in clinical settings including test speed, sensitivity, specificity, affordability and ease of use. The antibody-functionalized PAM serves as a tightly localized solid-phase support structure where ubiquitous solid-phase immunoassay chemistries can be applied for clinical and lab use. The microchannel format shown in Figures 1-3 helps overcome common mass-transfer limitations by convective transport of target organisms to the solid-phase surface and prolonged interaction with the surface due to size exclusion. Overcoming mass-transfer limitations in this manner is only effective if non-specific interactions of interfering species and reporter molecules are mitigated as in the case here with the hydrophilic PAM surface chemistry. We developed the functionalizable PAM by copolymerizing acrylamide monomer with streptavidin acrylamide, enabling subsequent generic attachment of biotinylated antibodies to the porous monolith. An alternative option is to instead directly graft an antibody acrylamide during the initial PAM fabrication. PAM was fabricated inside a low-cost glass-polymer chip. The microchannels were first defined using patterned UV-polymerization of a 300 μm thick layer of urethane diacrylate sandwiched between two acrylate-silanized glass coverslips (Abhyankar and Hatch 2012). Under our current experimental conditions, this technique allows quick prototyping of microfluidic devices with critical features larger than 200 μm. PAM was fabricated inside the device with branching channels on either side for flexible delivery of different fluids including reporter reagents, buffer and waste to or away from the monolith.

Functionalization of PAM was performed by subsequent incubation of biotinylated capture antibodies. Figure 4A-B demonstrates strong fluorescent signal from a PAM after incorporation of fluorescent Atto 488-biotin molecules, as compared to the negative control PAM fabricated without streptavidin-acrylamide.

To characterize transport characteristics of the device, different size fluorescent beads were injected through the device with flow through the PAM at 2 μl/min. Beads flowed uniformly across the full width of the PAM element and no side wall leakage was observed,

demonstrating that the PAM was sufficiently grafted to the glass/UDA channel walls. A PAM filter with pore sizes small enough to exclude target bacteria is advantageous for focusing and concentrating the bacteria and facilitating rapid and efficient binding to the antibody-coated PAM surface. Larger pore sizes are advantageous to reduce pressure for a given flow rate, and help minimize clogging of pores or blocking of the reactive surface by non-targeted species in the sample. Optimizing for both criteria, the PAM monolith had a limiting pore size between 0.2- 1.0 μm, which is evaluated based on the passage of different size beads; 100 and 200 nm beads passed but not 1 μm beads as shown in Figure 4C-E. The slower flow rate of beads within the PAM than in the open channel results in a dramatically higher concentration of beads, even those that can pass through the monolith within the PAM under continuous flow (Figure 4C-D). In Figure 4E, 1 μm beads are clearly excluded and accumulate at the front edge of PAM. This pore size allows effective filtering of rickettsiae bacteria cells (1 μm × 4 μm) while permitting smaller particulates and macromolecules in serum or lysed blood sample to flow through, and maximizing the efficiency of immunoreactive capture of rickettsiae at the PAM surface.

3.2 Dose response of *R. typhi* detection

Serum and blood spiked with *R. typhi* were used as model biofluids for evaluation of device performance as the assay format was developed. The assay protocol is illustrated in Figure 3 and described in Material and methods. The PAM functionalized with polyclonal anti-*typhi* antibodies captured the targeted rickettsial organisms with high efficiency, ~100%, as determined by fluorescence imaging. The captured *R. typhi* at the front edge of the PAM was stained with AF 647-labeled polyclonal anti-*typhi* antibodies. The imaged fluorescent particle count increased linearly with known concentrations of spiked cells. When target is below 100 cells, the captured *R. typhi* can be individually counted without too much overlap and within this range, the correlation between known concentrations and captured particles was ~1:1.

Typical fluorescent images of the PAM by the end of the assays are shown in Figure 5A-F. For samples with low concentration of rickettsiae, fluorescent particles of the labeled bacteria can be individually counted from the PAM images by automatic particle analysis software yielding results equivalent to manual counting, with detection limit at <10 cells/100 μl. In Figure 5B, 7 fluorescent particles were identified for a condition where 6 were expected on average; note that sampling from the known stock concentration does not allow exact prediction of the number of particles loaded for each assay. Figure 5C shows an example where 66 fluorescent particles were counted, where 60 were expected on average. Low non-specific fluorescent background as the backdrop to fluorescently stained particles allows accurate counting of particles by setting a fluorescent intensity threshold based on negative control. For samples with concentration over 1×10^4 cells/ml (667 cells loaded), captured fluorescent particles were not individually resolved in the fluorescent images. In these cases, estimated number of fluorescent particles was calculated from the total number of fluorescent pixels within the 100 μm × 25 μm detection window at the front edge of the monolith divided by an average fluorescent particle size. By this metric, the increase in fluorescent signals increased linearly with respect to rickettsiae concentration before the signal reaches a spatial saturation plateau above 10^5 cell/ml. (Figure 5G).

Using an unfunctionalized PAM, only 78 rickettsiae cells were detected from 60 μl 1×10^5 cells/ml sample where 6000 cells were loaded, corresponding to a 1.3% retention rate, presumably caused by non-specific trapping of the bacteria inside the porous polymer structure. The great majority of the rickettsial organisms (>98%) were rinsed away, indicating low-fouling property of the polyacrylamide backbone of PAM, which is important for highly sensitive and specific pathogen capture.

Although individual particles are effectively counted here with imaging, a simplified point detection scheme to measure the total fluorescence signal from the detection zone is desirable for more affordable and compact portable instrumentation when compared with a CCD imaging setup. The sensitivity of point detection is directly dependent on the level of non-specific background signal and size of the detection zone. To evaluate point detection, the averaged signal of the full detection zone encompassing the capture region at the front edge of the monolith (e.g., as illustrated in Figure 2C) is calculated from the fluorescent images and plotted as a function of target cells loaded in Figure 5H. Using the point detection method, the detectable level (calculated as background plus three times of noise variation) is increased compared to particle counting, but is still quite good at ~10 cells from 60 μl lysed blood samplea and 25 cells from 60 μl serum samples. This excellent point detection sensitivity is attributed to the low non-specific background along with small zone of detection achieved with the hydrophilic monolith exclusion approach. When >10,000 cells were captured, the fluorescent signal was saturated for the same detector settings as the surface of the PAM was densely covered by captured rickettsiae (Figure 5F).

3.3 *R. typhi* detection in lysed blood

Because *Rickettsia* is an intracellular parasite and may largely reside in circulating endothelial cells and white blood cells, a clinical whole blood sample may require lysing of circulating host cells to release the bacteria. We found that 4 volumes of 0.2% Saponin is effective in breaking up most of the blood cells while maintaining the basic structure of rickettsiae (Siddiqui et al. 1979), allowing subsequent immunofluorescent staining of the bacteria captured on the PAM. However, since there is still debris in the blood lysate, we found that a pre-filtering step using a glass fiber filter helped to prevent downstream clogging at the PAM assay filter. Dose response of *R. typhi* detection from whole blood is illustrated in Figure 5G-H. The results demonstrate fast and sensitive rickettsiae detection from whole blood using the PAM device with simple sample preparation steps of blood lysis with detergent and membrane filtering.

3.4 Specificity test with *R. typhi, R. conorii* and *E. coli*

To demonstrate the specificity of the assay for R. typhi detection, we performed assays using serum spiked with the same concentration (1×10^4 cells/ml) of *R. typhi, R. conorii*, and *E. coli O157:H7* using the same anti-*R. typhi* functionalized PAM devices. The result shown in Figure 6 demonstrates that compared to equivalent levels of specific target, the signal drops 92% when the same concentration of related species *R. conorii* is present, and the signal drops to background noise when the same concentration of *E. coli O157:H7* is present. The specificity of an individual assay element is largely dependent on the specificity of both the capture and the reporter antibody. In addition, the specificity of the

assay may also be further improved by optimizing the pore size to avoid non-specific trapping of particles and by more stringent rinsing. Furthermore, the layout of the microfluidic device can be expanded for multiplexed assays targeting several different related bacterial species simultaneously.

4. Conclusions

We have developed a polyacrylamide monolith-based fluidic device for detection of a SFG and TG rickettsiae in serum and blood samples. The porous hydrophilic monolith functionalized with anti-*R. typhi* antibody can effectively capture the bacteria from serum and blood specimen and allow subsequent immunofluorescent staining and imaging of the bacteria inside the chip. The assay can handle 10 to >100 μl of sample and high sensitivity can be achieved in about 30 min for 10 μl samples. The detection limit is $\sim 10^2$ cells/ml with ~100% capture rate. Dynamic range of detection covers 4 orders of magnitude, from 100 cells/ml to 5×10^5 cells/ml. This is a novel approach aiming towards a fully automated point-of-care diagnostic system for rapid and sensitive detection of rickettsiae and other blood-borne bacterial pathogens.

Acknowledgements

References

Abhyankar VV, Hatch AV. Advanced Healthcare Materials. 2012; 1:773–778. [PubMed: 23184830]

Azad AF. Clinical Infectious Diseases. 2007; 45:S52–S55. [PubMed: 17582570]

Birg M-L, La Scola B, Roux V, Brouqui P, Raoult D. Journal of Clinical Microbiology. 1999; 37:3722–3724. [PubMed: 10523584]

Chapman AS. Diagnosis and Management of Tickborne Rickettsial Diseases: Rocky Mountain Spotted Fever, Ehrlichioses, and Anaplasmosis - United States. C. f. D. C. a. Preventions. 2006; 55:1–27.

Eremeeva ME, Dasch GA, Silverman DJ. Journal of Clinical Microbiology. 2003; 41:5466–5472. [PubMed: 14662926]

Gury a V, Mechref Y, Palm AK, Michálek J, Pacáková V, Novotný MV. Journal of Biochemical and Biophysical Methods. 2007; 70:3–13. [PubMed: 17254635]

Jiang JU, Temenak JJ, Richards AL. Annals of the New York Academy of Sciences. 2003; 990:302–310. [PubMed: 12860643]

La Scola B, Raoult D. Journal of Clinical Microbiology. 1996; 34:2722–2727. [PubMed: 8897172]

Moody AH, Chiodini PL. Clinical & Laboratory Haematology. 2000; 22:189–201. [PubMed: 11012630]

Namera A, Nakamoto A, Saito T, Miyazaki S. Journal of Separation Science. 2011; 34:901–924. [PubMed: 21394910]

Nyka W. Journal of Infectious Diseases. 1950; 86:81–87. [PubMed: 15402293]

Palm A, Novotny MV. Analytical Chemistry. 1997; 69:4499–4507.

Quesada M, Sanfeliu I, CardeÑOsa N, Segura F. Annals of the New York Academy of Sciences. 2006; 1078:578–581. [PubMed: 17114782]

Siddiqui WA, Kan SC, Kramer K, Richmond-Crum SM. Bull World Health Organ. 1979; 57(Suppl 1): 75–82. [PubMed: 397010]

Stenos J, Graves SR, Unsworth NB. The American Journal of Tropical Medicine and Hygiene. 2005; 73:1083–1085. [PubMed: 16354816]

Svec F. Journal of Chromatography A. 2010; 1217:902–924. [PubMed: 19828151]

Vázquez M, Paull B. Analytica Chimica Acta. 2010; 668:100–113. [PubMed: 20493286]

Walker DH. Clinical Infectious Diseases. 1995; 20:1111–1117. [PubMed: 7619984]

Xie S, Svec F, Fréchet JMJ. Journal of Polymer Science Part A: Polymer Chemistry. 1997; 35:1013–1021.

Highlights

- Capturing bacteria via monolith in a micro-flow channel overcomes transport issues;

- Bacteria from blood volumes up to100 μl were captured and stained within minutes;

- Hydrophilic monolith offers low non-specific fouling, enhances detection sensitivity;

- Packing captured bacteria into microscale imaging area enhances detection sensitivity;

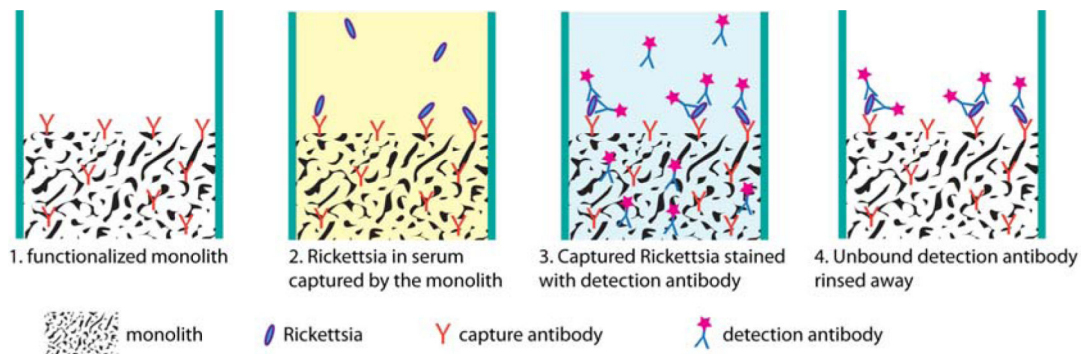- Fewer than 10 *Rickettsia typhi* cells were detected in blood with ~100% capture rate.

Figure 1. Schematic illustration of rickettsiae assay format
1. Polyacrylamide monolith (PAM) functionalized with anti-rickettsiae capture antibodies.
2. As sample flows through the monolith, rickettsiae cells are excluded by smaller pore size and specifically captured by antibodies at the monolith edge. 3. Captured rickettsiae cells are stained by fluorescently labeled reporter antibodies. 4. Final rinse leaves fluorescently tagged rickettsiae for quantitative measurement.
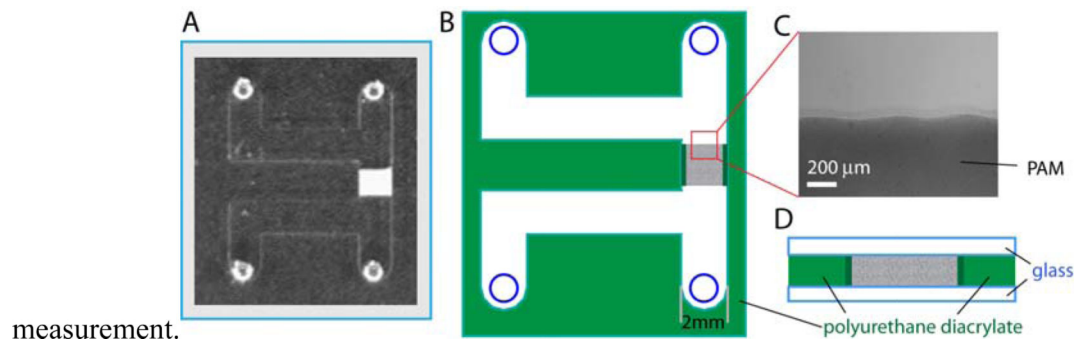
measurement.

Figure 2. Structure of the PAM microfluidic device
The channel layout (300 μm deep 2 mm wide) and PAM filter are sequentially formed by *in situ* photolithographic polymerization of polyurethane diacrylate and PAM between two glass coverslips. (A) Bright field device image. (B) Top view of the device layout. (C) Bright field image of the PAM edge. (D) Side view of the PAM structured inside the channel.
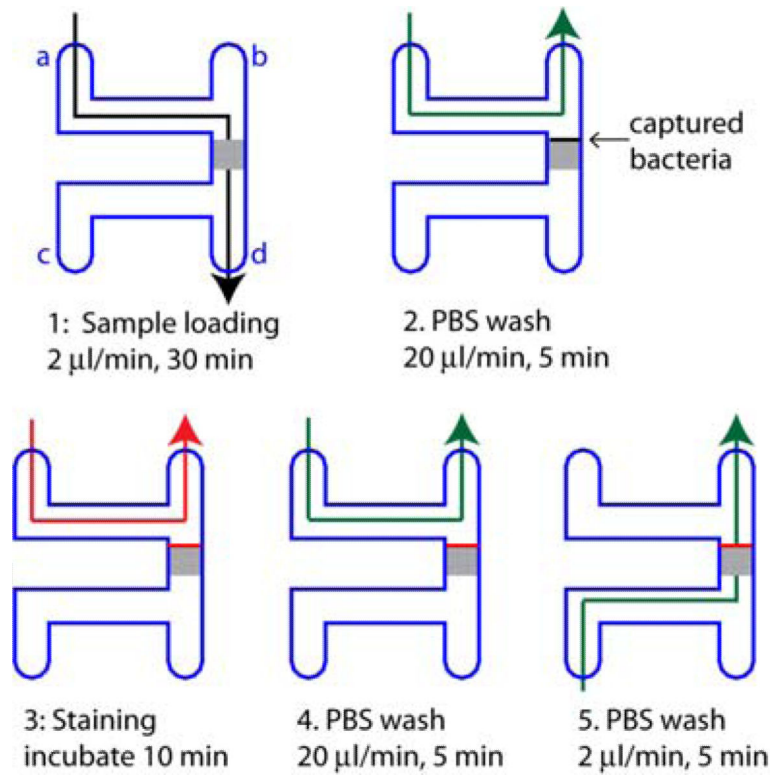
Figure 3.
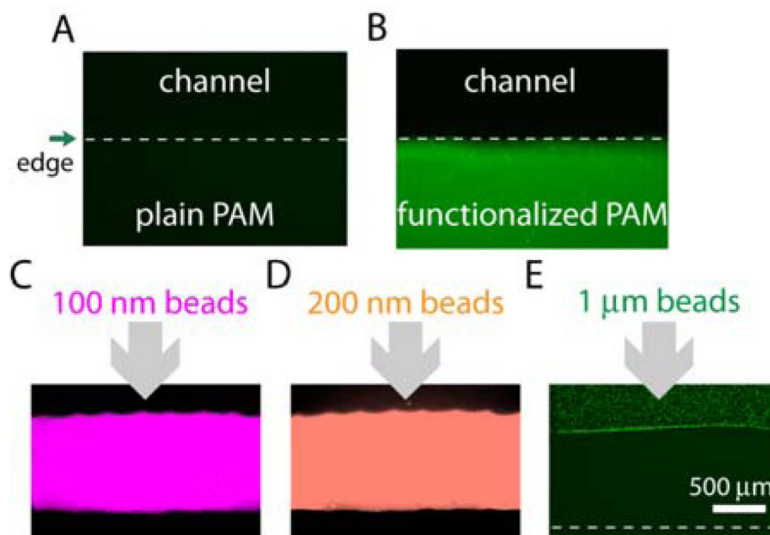Assay protocol for *R. typhi* detection from serum or filtered blood lysate sample.

Figure 4. Characterization of PAM functionalization and pore size
(A-B) Pseudo-colored fluorescent images of plain PAM and functionalized PAM, which is co-polymerized with streptavidin acrylamide, after staining with fluorescent Atto 488-biotin. Strong fluorescence inside the functionalized PAM indicates successful integration of the streptavidin moiety. (C-E) Pseudo-colored fluorescent images of PAM when fluorescent beads of different sizes are injected from the upper side of the PAM. In C and D, 100 nm red and 200 nm orange fluorescent beads can flow through and stain the entire monolith. In E, 1 μm green fluorescent beads are blocked at the front edge of the monolith.
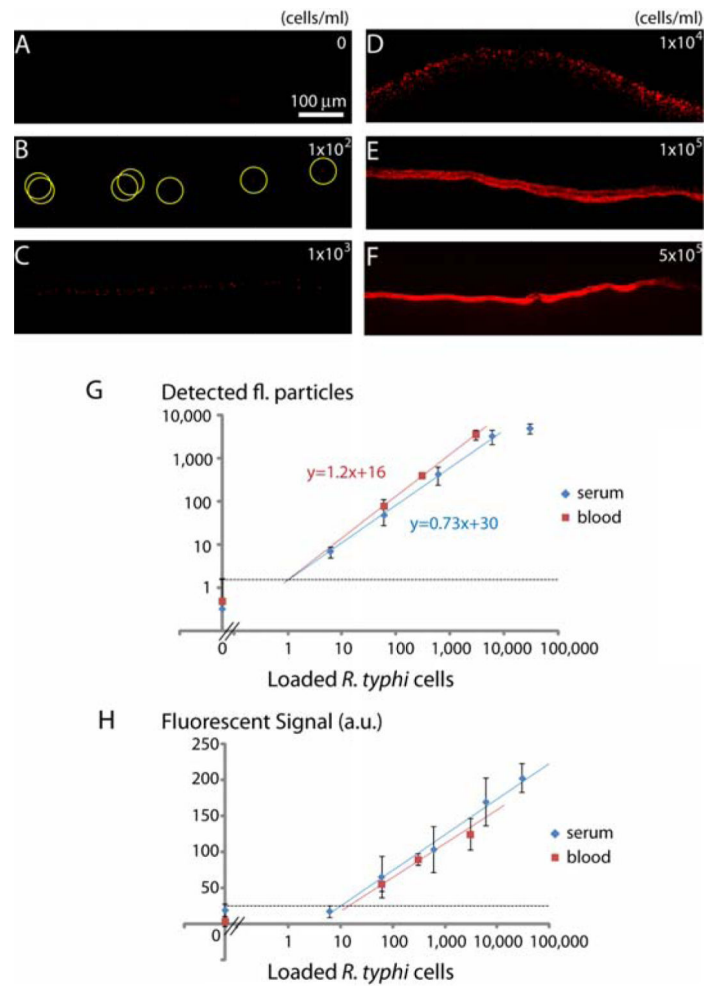
Figure 5. Dose response of *R. typhi* detection
(A-F) Pseudo-colored fluorescent images of the front edge of PAM after the assays with 60 μl serum or lysed blood sample spiked with increasing concentration of *R. typhi* using PAM conjugated with anti-*R. typhi* antibodies. Fluorescent particles in figure B are highlighted with yellow circles. (G) Fluorescence imaging ananlysis comparing particle counts to number of cells expected in the loaded sample. (H) Simpler point-detection analysis; averaged fluorescent signal across the PAM region of interest vs. expected concentration of *R. typhi* in serum and lysed blood sample. Error bars are standard error of the mean from three independent experiments. The dotted line indicates the detection limit for lysed blood sample.
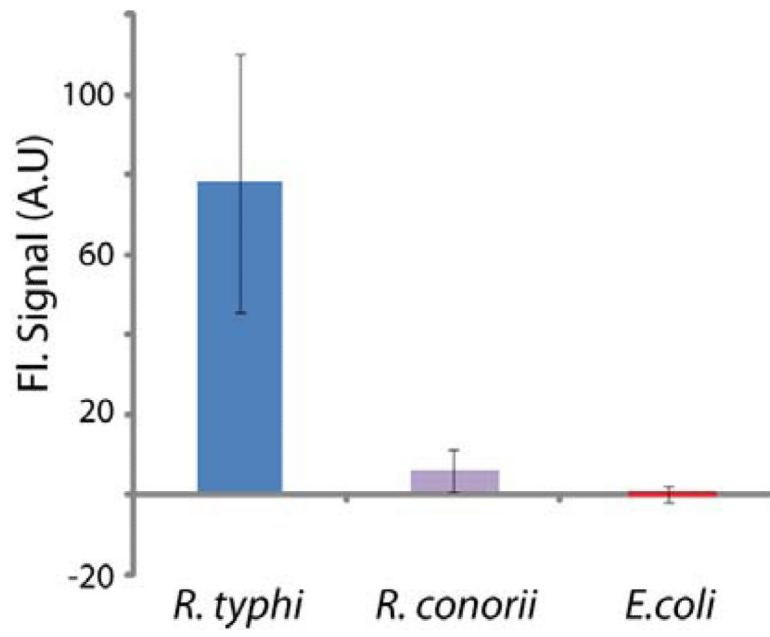
Figure 6. Detection specificity
Averaged fluorescent signal from assays using serum sample spiked with 1×10^4 cells/ml *R. typhi, R. conorii* or *E. coli O157:H7* with anti-*R. typhi* PAM and anti-*R.typhi* detection antibodies. Error bars are standard error of the mean from three independent experiments.